Characterizing the Topside Bulge in the Ionosphere of Mars

Table of Contents

The purpose of this investigation is to characterize a poorly-understood and variable feature of the topside ionosphere and to test possible explanations for its existence. This feature is important because its properties affect atmospheric escape of ions like HCO^+ that impact the loss rate of water and therefore can improve our understanding of the evolution of Mars' atmosphere.

1 – Introduction to the Ionosphere of Mars

The ionosphere is the ionized region of an atmosphere. In this region, the properties of ions and electrons (referred to as plasma) are important since they vary due to solar drivers [e.g., *Withers*, 2009], the local magnetic field environment [e.g., *Duru et al.*, 2006], and phenomena occurring in the neutral atmosphere [e.g., *Bougher et al.*, 2000]. The ionosphere of Mars forms where solar photons that are capable of ionizing neutrals are absorbed (80 – 400 km). The top of the ionosphere shares a boundary with shocked solar wind plasma, making this region subject to numerous escape processes.

An ionospheric profile – the variation in electron number density with altitude – offers insight to various physical processes that produce and move plasma. A density peak called the M2 layer forms near 130 km due to absorption of solar EUV photons. Below ~150 km the ionosphere is well described by photo-ionization and chemical reactions. Above ~150 km, the timescale for transport becomes smaller than the chemical timescale and plasma becomes subject to motion due to local forces. Plasma density decreases with altitude above the peak and observations have shown the topside to have significant density enhancements at times (Figure 1). One recurrent topside feature is the appearance of a bulge between 150 and 200 km [*Withers et al.*, 2012].

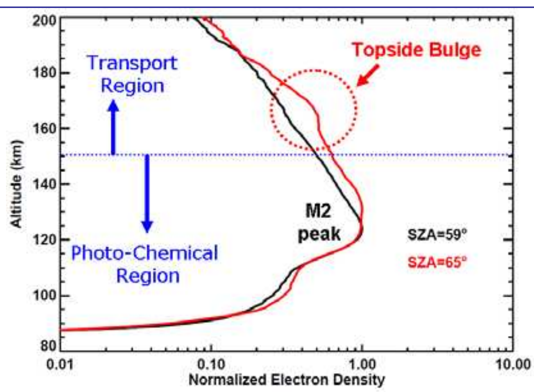

Figure 1. Ionospheric profiles of Mars. The number of electrons per unit volume is normalized to the maximum value and plotted as a function of altitude as measured by the radio science experiment (MaRS) on MEX for different solar zenith angles. A peak (M2) layer forms due to solar EUV absorption. Below 150 km the ionosphere is described by photo-chemical production and loss. Above 150 km, plasma moves subject to local forces. Why a sporadic topside layer (bulge) appears has yet to be determined.

Ions such as HCO^+ and HCO_2^+ are abundant at topside altitudes [*Matta et al.*, 2013a]. Enhancements in their densities affect the rates at which they recombine to produce H, a light atom that can easily escape Mars' atmosphere by a variety of non-thermal escape processes [e.g., *Shizgal and Arkos*, 1996]. Furthermore, plasma transport is sensitive to density gradients, making topside structures key triggers for increasing the thermal escape of ions. Due to the relatively complex nature of the topside ionosphere and to the lack of comprehensive *in situ* measurements of plasma and field properties, this region has been poorly investigated. As a result, characteristics of the topside ionosphere as well as sources responsible for its intermittent enhancements remain unknown.

2 – Objective and Outline of Proposed Investigation

Significant plasma variability has been observed in the topside ionosphere of Mars [*Withers et al.*, 2012]. The motivation behind the proposed work is to find plausible mechanisms to explain these variations and to interpret their effects on the atmosphere. Spacecraft observations of the upper ionosphere have revealed a recurring feature referred to as the topside bulge. This feature was first discovered in one of the two *in situ* observations made by the Viking Landers [*Hanson et al.*, 1977], shown in Figure 2, and was subsequently detected in ~10% of radio occultation observations [*Wang and Nielsen*, 2003] and ~60% of topside sounder observations [*Kopf et al.*, 2008].

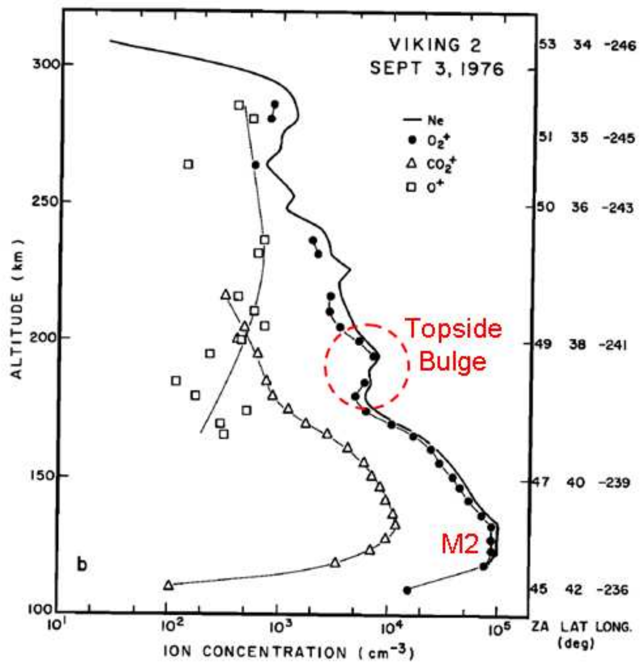

Figure 2. First observation of a topside bulge measured by Viking Lander 2, from [Hanson et al., 1977]. The local plasma density enhancement between 180 and 200 km shows a ~20 km wide layer with a local peak that is nearly a factor of 10 smaller than that of the main peak (M2) density.

The topside ionosphere is a key region of the atmosphere since it contains plasma that is closer to the ionopause (the ionospheric boundary with outer space) and so these plasma particles are more susceptible to escape than those in the lower ionosphere. Also, a great deal of insight into plasma dynamics can be obtained by investigating the mechanisms that govern this region. Variations in the plasma densities in any region of the ionosphere result in variations in the properties of propagating radio signals and can impact communications as well as the yield of scientific experiments. Therefore, understanding the topside ionosphere is beneficial for both scientific and operational applications.

Viking Lander ion density measurements were analyzed using *a priori* assumptions of neutral composition [*Nier and McElroy*, 1977; *Hanson et al.*, 1977]. Results showed an ionosphere made of O_2^+, O^+ and CO_2^+ and did not account for the presence of the bulge. Subsequent studies of escape considered only oxygenated ions [e.g., *Ma and Nagy*, 2007]. More recent observations have shown the neutral atmosphere to contain molecular hydrogen [*Krasnopolsky and Feldman*, 2001]. H_2 is a very reactive species, so its presence leads to the production of hydrogenated ions (those containing at least one atom of hydrogen), with comparable densities to those measured by Viking as shown in Figure 3 [*Matta et al.*, 2013a]. Two such ions, HCO^+ and HCO_2^+, recombine with electrons to produce H. Therefore, determining how topside plasma density enhancements of hydrogenated ions affect their transport is important for understanding the evolution of both constituents of water and its related escape rate from the planet.

Figure 3. The noon-time ion composition of the Martian ionosphere simulated with an ionospheric model that used the Viking Lander neutral composition as well as more recent measurements of H_2. The shaded region between 150 and 200 km that is the region of interest of this work shows the hydrogenated ions HCO^+ and HCO_2^+ to be more abundant than O^+. This affects calculations of water escape rates. Figure and ionospheric model description are in Matta et al., [2013 b].

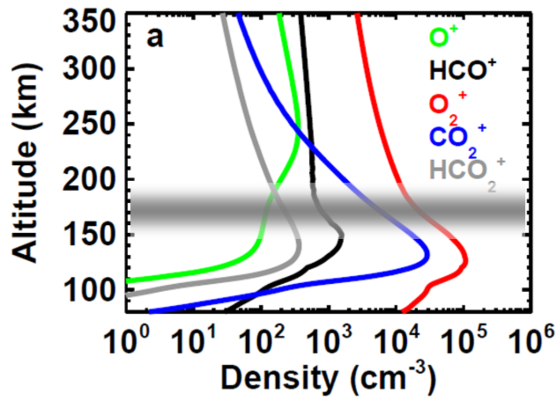

The goal of this project is to characterize the bulge feature in the topside ionosphere of Mars between 150 and 200 km. This work steps away from the rigorously studied lower ionosphere and focuses on a critical region of the ionosphere of Mars that is poorly understood at present. Data from three instruments: Mars Global Surveyor radio subsystem, Mars Express radio subsystem, and Mars Express topside ionospheric sounder (MARSIS) as well as existing tools will be utilized for the following scientific objectives:

Objective 1: Use the three datasets to determine properties of the bulge such as altitude, magnitude, width, timescale, and occurrence rate. Determine correlations between bulge observations and crustal field properties. Analyze these results to characterize the variability of the bulge with location, solar zenith angle, season and solar cycle.
Objective 2: Derive the effects of introducing a topside enhancement on plasma transport velocities, using the observed properties of the bulge. Interpret these velocities in the context of existing estimates of thermal and non-thermal escape speeds of ions.
Objective 3: Identify any systematic differences in bulge characteristics between data sets.
Objective 4: Use observed bulge properties to investigate source processes likely to produce such topside enhancements by considering contributions from chemical mechanisms (recombination), solar mechanisms (solar wind electron impact ionization), and magnetic effects (strong crustal fields) utilizing an existing model.

To recap, the topside ionosphere is a critical part of the atmosphere that is accessible to spacecraft, subject to solar wind interactions, and sensitive to escape mechanisms, yet it remains one of the most poorly characterized regions of the Martian ionosphere. The significance of each scientific objective will result in improving our current understanding of this key region of the ionosphere of Mars. The resulting investigations will have implications for atmospheric escape and its evolution and are important for forming predictions for the measurements of upcoming missions.

3 – Status of Current Research on the Topside Ionosphere of Mars

The topside ionosphere of Mars (above ~150 km) is a region above the peak where the timescale for particle diffusion is smaller than the timescale for chemical interactions. As a result, ions and electrons can drift due to the forces generated by plasma pressure gradients, plasma temperature gradients, gravity, and friction from inter-particle collisions [*Schunk and Nagy*, 2009]. Other mechanisms such as induced currents or magnetic fields can also affect ion and electron motion [e.g., *Shinagawa and Cravens*, 1989]. The dearth of comprehensive *in situ* measurements in those regions has resulted in a more theoretical determination than a data-driven understanding of the physical processes that affect the plasma in the Martian topside ionosphere.

Radio occultation experiments (on board the Mariners 4, 6, 7 and 9, Viking Orbiters 1 and 2, Mars Global Surveyor and Mars Express spacecraft) as well as the MARSIS topside radar sounding experiment (on Mars Express) are the two methods to date that have been used on flyby and/or orbiting spacecraft to measure ionospheric structure as a function of altitude. Only two *in situ* measurements of the ionosphere have been made to date by the Viking 1 and 2 Landers [*Hanson et al.*, 1977].

Several distinct features have been more recently observed in the topside ionosphere of Mars. One such feature is the topside bulge (also referred to in the literature as the second topside layer [*Kopf et al.*, 2008] or the M3 layer [*Pätzold et al.*, 2007]). This is a large scale (≥10 km wide) enhancement in electron density that appears above the peak. In some profiles, multiple bulges appear [*Wang and Nielsen*, 2003] as shown in Figure 4.

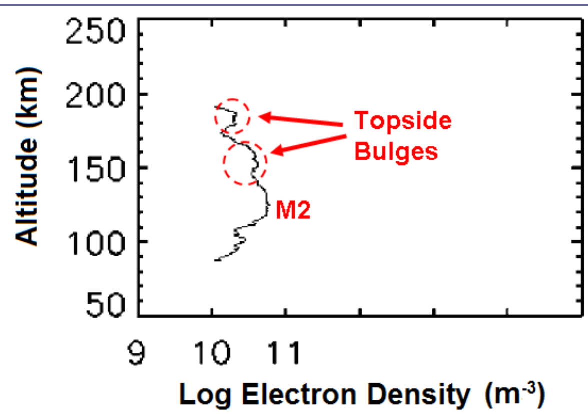

Figure 4. MGS near terminator (dusk) radio occultation profile revealing two bulges in the 150-200 km range above the peak M2 layer. The first enhancement above 150 km is only a factor of 2 smaller than the M2 peak layer density. Figure adapted from Wang and Nielsen [2003].

Following the Viking Lander 2 observation of the bulge, the Viking Orbiter measurements revealed this feature in only a fraction of the total (~60) radio occultation observations [*Ness et al.*, 2000]. More recently, the topside ionospheric bulge was detected with a higher frequency (~10%) by Mars Global Surveyor radio occultation measurements of the near-terminator (dusk) ionosphere [*Wang and Nielsen*, 2003]. From the Mars Express Radio Science experiment, ~10% of radio occultation profiles showed an increase in the electron number density between 160 and 180 km [*Withers et al.*, 2012]. This feature was attributed to either external interactions with the solar wind or to large changes in the internal mechanisms that produce the ionosphere at those altitudes.

The Mars Express subsurface and ionospheric sounder (MARSIS) measured the electron number densities from the location of the orbiting spacecraft down to the peak [*Gurnett et al.*, 2005]. The MARSIS top-side ionospheric sounder is not limited by occultation geometry and so can observationally cover a larger range of solar zenith angles than was available from radio science experiments. As shown in Figure 5, the topside bulge was detected at a higher frequency in the near sub-solar ionosphere (~60% of the measurements) and at a comparable frequency to radio occultation detections closer to the terminator (~5%) and was found to occur at slightly higher altitudes (between 180 and 240 km) than observed by radio occultations [*Kopf et al.*, 2008].

Figure 5. The probability of occurrence of the second layer (topside bulge) in MARSIS topside sounder observations from one month of observations spanning August 5th – September 5th, 2005. Figure adapted from Kopf et al. [2008].

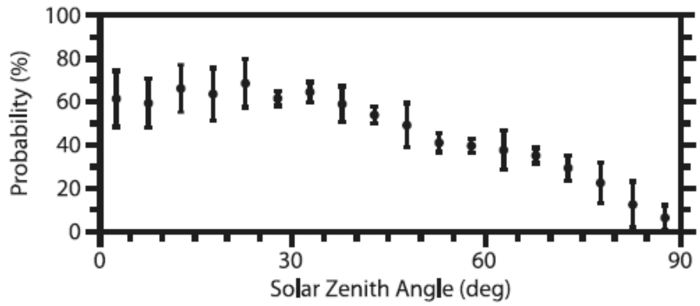

The topside bulge has additionally been attributed to other possible sources such as interactions with a dynamic magnetic field [*Shinagawa and Cravens*, 1992], transition from photochemical to transport region in the ionosphere [*Nagy and Cravens*, 2002], wave activity [*Wang and Nielsen*, 2003], chemical build up of O^+ [*Kopf et al.*, 2008], or to large plasma temperature enhancements that decrease the rate at which ion-electrons pairs recombine, resulting in a pile up of plasma at those altitudes [*Fox and Yeager*, 2006].

Previous work was conducted at Boston University (BU) to simulate ion composition in the topside ionosphere and to study the effects of plasma temperature enhancements as well as those of fluctuating local magnetic field environments on the plasma structure of the ionosphere [*Matta*, 2013]. It was found that several of the mechanisms suggested in the literature (such as O^+ layer formation, photochemical to transport region transition, increasing plasma temperature, and local magnetic field morphology) could not sufficiently explain the formation of these topside bulges [*Matta et al.*, 2013a, b].

Of the possible mechanisms suggested as responsible for forming the topside ionospheric bulge, interactions with the solar wind along open field lines (those that originate at the surface and culminate in the inter-planetary magnetic field) remain the most likely candidates for sources that produce this structure. Energetic electrons from the solar wind can precipitate into the ionosphere along open field lines [*Lundin et al.*, 1991; *Krymskii et al.*, 2002; *Lillis et al.*, 2008]. Several of these precipitating electrons have sufficient energy to ionize neutral particles in the topside ionosphere. This mechanism for enhancing topside plasma is plausible since it is consistent with the recently observed sporadic nature of the topside bulge feature whereas other mechanisms predict more global and ubiquitous features that are not consistent with observations.

An investigation of the occurrence rate of the topside bulge for a span of ~20 months of MARSIS topside sounder observations showed that the bulge occurs more frequently in regions of weak or no crustal magnetic fields [*Kim et al.*, 2012]. This result competes with what the theoretical mechanisms have suggested [e.g., *Krymskii et al.*, 2002], and cannot reconcile the possibility that solar wind electron precipitation is a likely source. The disagreement found between limited observations and theories for source mechanisms likely to produce a topside plasma enhancement emphasizes the need to thoroughly investigate and characterize this region of the ionosphere.

To date, Mars Global Surveyor Radio Science (MGS RS), Mars Express Radio Subsystem (MEX MaRS) and MEX Advanced Radar for Subsurface and Ionosphere Sounding (MARSIS) observations have shown that a topside ionospheric bulge is a recurring feature in the ionosphere. This feature has not yet been rigorously characterized and theoretical possibilities of the mechanisms that form this bulge have been inadequate. This project aims to address these shortcomings and to improve our understanding of both the properties and sources for forming the topside bulge in the ionosphere of Mars. The consequences of topside plasma enhancements on ion composition and dynamics will be investigated to assess their impacts on ion escape.

4 – Dataset Availability and Risk Assessment

This study will use three publicly available datasets retrieved from the NASA Planetary Data System and the European Space Agency's Planetary Science Archive:

Dataset I: The full set of 5600 radio occultation profiles obtained by the MGS RS experiment is available at: http://atmos.nmsu.edu /PDS/data/mors_1102. This dataset provides the electron number density as a function of altitude between 80 and 200 km for a range of observational conditions. This includes the range of interest for this study (between 150 and 200 km). The lifetime of the MGS mission provided a dataset that is well suited for seasonal and solar cycle variability studies.

Dataset II: Frequency residuals from ~600 daytime radio occultation profiles obtained by the MEX MaRS experiment are publicly accessible on the Planetary Science Archive available at: http://psa.esac.esa.int:8000/aio/jsp/fileXML.jsp?DATA_SET_ID=MEX-M-MRS-1/2/3-EXT2-2011-V1.0&return_type=Tree. Only a subset of these measurements has been archived as electron density profiles. To transform frequency residuals into electron density profiles, tools which have already been developed and validated at Boston University (BU) will be employed, as shown in Figure 6 [*Moore et al.*, 2012; *Withers et al.*, 2013]. Due to MEX's elliptical orbit, the ionospheric profiles available from this dataset cover a wider range of altitudes (80 – 350 km) than MGS. Fortunately, the MEX and MGS radio occultation datasets overlapped for a few months. This will allow for comparative observations of the ionosphere by both spacecraft using similar observational techniques.

Dataset III: The MARSIS topside sounder radar measurements are available in the forms of ionograms on the PDS and are available at: http://psa.esac.esa.int:8000/aio/jsp/

metadata.jsp?DATA_SET_ID=MEX-M-MARSIS-3-RDR-AIS-EXT1-1.0&RETURN_TYPE=HTML. Ionograms have a distinctive signature for the second peak (topside bulge) and tools have already been developed and published to extract the observational properties of the bulge from this dataset [*Zou et al.*, 2010]. Collaborator Morgan from the MARSIS team at the University of Iowa will provide feedback when needed to validate the data extraction results. Nearly 100,000 topside sounder measurements have been made. This study will use the daytime observations (solar zenith angle ≤85°) made when the spacecraft was orbiting below 600 km and that have continuous sounding data with at least one cusp (indicating a topside layer). These conditions result in a dataset of ~5500 topside sounder profiles. MARSIS observations with similar conditions to radio occultation measurements will be used for comparisons of different techniques.

This work will use only publicly accessible datasets in addition to various software tools necessary to manipulate the data. The data presently available online is adequate and sufficient for this study. Tools necessary to extract the quantities needed for the proposed data analysis have all already been developed either in-house (at BU) [*Fallows et al.*, 2011; *Moore et al.*, 2012; *Withers et al.*, 2013] or have been made publicly available [*Zou et al.*, 2010]. Aside from only minor adjustments to these utilities, no new tools will need to be developed, minimizing risk due to software development delays.

Figure 6. Proof of concept for derivation of electron density profiles at BU from both MGS (left) and MEX (right) frequency residual data. The BU-derived profiles (black) are compared to archived values from the Planetary Data System (red). The derivation methods and comparisons with existing data are in Moore et al. [2012]; Withers et al. [2013].

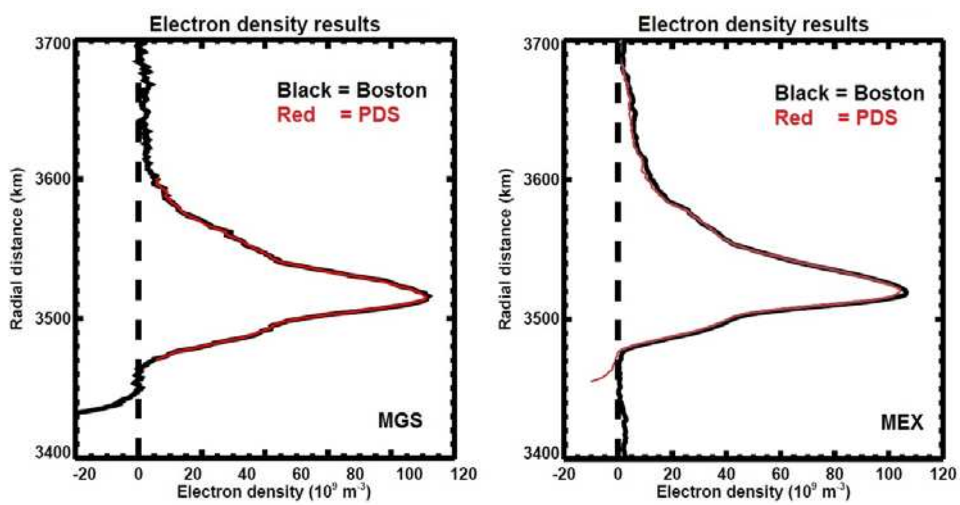

5 – Task A: Locating and Extracting the Topside Bulge Features

Meeting the scientific objectives requires a systematic method of locating the topside bulge feature in observations from the three datasets and of extracting the altitude, magnitude and width of this feature. Data from each instrument used in this investigation were returned from varying regions of the ionosphere; however, the electron density measurements between 150 and 200 km are common to all datasets.

There are several thousand radio occultation observations to comb through. An automated tool for layer fitting, demonstrated in Figure 7, has been developed at Boston University. This tool was used to systematically determine the sporadic M1 layer that appears below the peak and has since been adapted for MGS, MEX and VEX observations. A series of steps will extract the properties of the topside bulge, beginning with the MGS radio occultation dataset, as follows:

Step A.1 – Adjust the altitude boundaries of the automated tool to include the topside bulge (with validation by manual inspection). If a peak is detected, the orbital properties of the spacecraft will be recorded. A Chapman function will be fit to the data to return the peak magnitude, altitude and width of the layer. A Chapman function is used for convenience here and not for physical reasons. Equally valid would be to use a Gaussian fit.

Step A.2 – Invert MEX radio occultation frequency residuals to electron density profiles.

Step A.3 – Repeat Step A.1 for the MEX radio occultation profiles.

Figure 7. Demonstration of the automated fitting tool used to detect layers in ionospheric profiles. The two dark blue points denote the adjustable altitude boundaries for fitting. Chapman functions are used to fit to the data for convenience. Other fits include Gaussian or Sine functions. This fitting routine provides the layer maximum density, altitude and width.

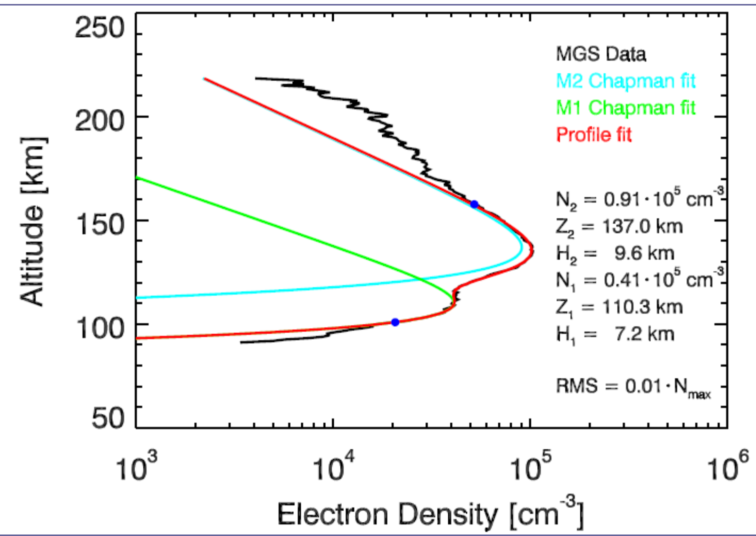

The MARSIS ionospheric sounder instrument dataset is provided as ionograms that are available on the public data archive. An ionogram is provided as a binary table and describes the spectral density of the radar signal as a function of frequency and time delay for the signal to make its round trip from the instrument to the ionosphere and back. A topside layer has a unique signature in this ionogram as shown in Figure 8.

The MARSIS ionograms have already been scanned for the topside feature according to the imposed restrictions (clear cusp, daytime profile). The bulge features will be located in the MARSIS ionograms as follows:

Step A.4 – Invert the ionogram data near the topside bulge to obtain the best fit width of the feature. Collaborator Morgan, a key MARSIS science team member in the University of Iowa, will offer advice on this process as needed. The mechanisms for making these inversions have already been developed and published [*Zou et al.*, 2010].

Step A.5 – Repeat Step A.1 for MEX MARSIS electron density profiles.
Step A.6 – Manually review atypical observations that failed automated detection.

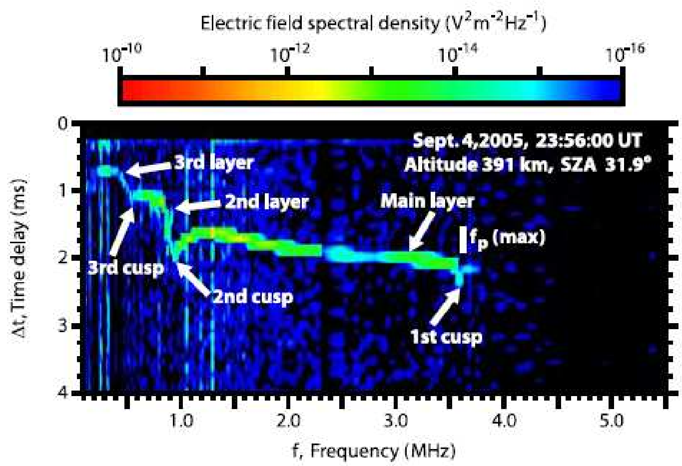

Figure 8. Figure from Kopf et al. [2008] that shows a sample ionogram measured by the MEX MARSIS topside ionospheric sounder. The electric field spectral density shows signal strength with frequency and time required for signal to be reflected back to the spacecraft (that is representative of altitude). The second and third cusps represent plasma enhancements above the peak of a topside bulge.

Results of this Task will provide us with the properties of the bulge, including: peak density altitude, peak density magnitude and layer width. The timescale may also be observed for a subset of the observations. These properties will be used to characterize the topside ionospheric bulge and to make correlations with observing conditions that are the focus of the next Task.

6 – Task B: Characterizing the Structure of the Bulge

The first and second scientific objectives of this work are to characterize the topside ionospheric bulge and to investigate any correlations with local and solar conditions. The transport dynamics resulting from variations in plasma gradients at the topside will be determined for comparison with thermal escape speeds and implications on ionospheric escape. Results from the observations of each dataset will be used be separately at first and then merged for comparison in the next Task. Beginning with the MGS radio occultation dataset, the steps required to complete this Task are:

Step B.1 – Statistically examine the topside bulge properties (altitude, magnitude, width). Retrieve local crustal field values from regions with bulge features. This will be done using the *Arkani-Hamed* [2004] spherical harmonics model that is based on MGS mangnetometer observations at 400 km. The crustal field model will then be used to determine local magnetic field properties such as strength and inclination angle with respect to the horizontal. The crustal field model demonstrated in Figure 9 has already been implemented by the Co-I for previous studies [*Mendillo and Withers*, 2008; *Matta* 2013, PhD Thesis]. Investigate correlations between bulge formation and latitude, longitude, solar zenith angle, local time, crustal field properties, season, and solar cycle and interpret these correlations (or lack of them). Repeat this analysis for locations where no distinct topside bulge was detected.

Step B.2 – Repeat Step B.1 for MEX radio occultation dataset.
Step B.3 – Repeat Step B.1 for MEX MARSIS topside sounder dataset.
Step B.4 – Characterize variations in transport velocities due to bulge density gradients.

The results of this Task will be compiled to develop characteristics of the topside bulge as measured by each instrument. These characteristics will be used to calculate the impact of pressure gradients (that are caused by this topside enhancement) on plasma transport velocities that push ions and electrons away from the bulge region. These results will also be used to address competing arguments for whether bulges form near strong or weak crustal magnetic field regions.

Figure 9. Two-dimensional projection of magnetic field morphology in a region of strong crustal [Mendillo and Withers, 2008] that can affect ionospheric plasma. The field orientation and strength are derived from the spherical harmonics model of Arkani-Hamed [2004] of magnetic field potential based on MGS measurements.

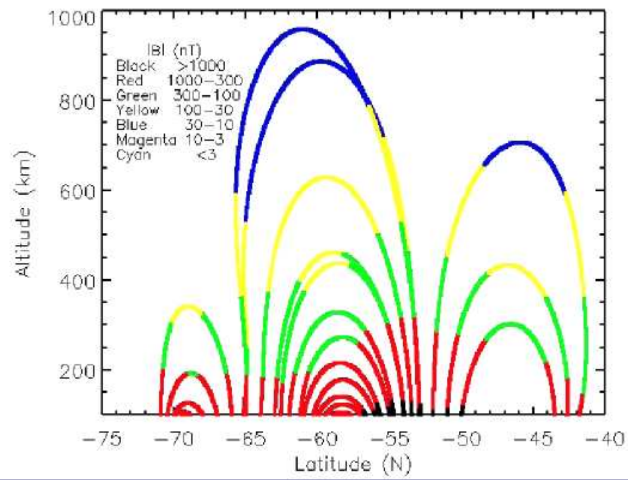

7 – Task C: Comparing Bulge Properties across Datasets

The third scientific objective is to identify any systematic differences in the three datasets used. The Task described here addresses this objective by inter-comparisons of the bulge characteristics derived from each dataset. As a result, the three datasets will be combined to compare the cumulative characteristics of the topside feature.

Step C.1 – Compare the bulge characteristics from the three datasets for overlapping as well as temporally distinct observations. Interpret the comparison results to establish a longer baseline of observations.

These unique comparisons for overlapping measurements from different instruments will be used to explain differences and agreements between measurement techniques.

8 – Task D: Interpreting Formation Mechanisms using Observations and Modeling

The final scientific objective of this proposal is to use the observed characteristics of the topside bulge to investigate the causes behind its production. Several mechanisms have been suggested to produce topside plasma enhancements, such as wave activity

[*Wang and Nielsen*, 2003] and plasma temperature variations [*Fox and Yeager*, 2006]. One theory attributes the bulge to a build up of O^+ [*Kopf et al.*, 2008], yet this can no longer be supported in light of new observations of H_2 that reacts quickly to reduce O^+ densities [*Krasnopolsky*, 2002; *Fox*, 2003; *Matta et al.*, 2013a]. Solar wind interactions can inject energy into the topside ionosphere and cause local neutral species to be ionized, and another theory states that such magnetic field interactions may be responsible for bulge production [*Shinagawa and Cravens*, 1992].

The remaining scientific objective of this investigation will be addressed in this Task by examining two mechanisms as potential sources for producing the topside bulge: (i) compositional changes of topside plasma and (ii) contributions of solar wind electrons precipitating along magnetic field lines. Modeling these two mechanisms as a proof-of-concept has been done to determine their candidacy as possible sources of plasma enhancements at bulge altitudes.

Photo-chemical byproducts other than O^+ may linger at bulge-altitudes. HCO^+ is a stable ion that builds up to appreciable quantities before reaching photochemical equilibrium [*Matta et al.*, 2013a]. Simulations of ion composition at sunset show that HCO^+ and CO_2^+ can form a distinct layer above the peak as shown in Figure 10. A topside layer appears due to diurnal variations in plasma temperatures. At cooler sunset conditions, ions recombine more slowly with electrons (at a rate that is inversely proportional to electron temperature raised to some power), resulting in slower removal of ion-electron pairs. The timescales for topside plasma recombination will be calculated and compared with observed timescales to determine their contribution to topside plasma structure.

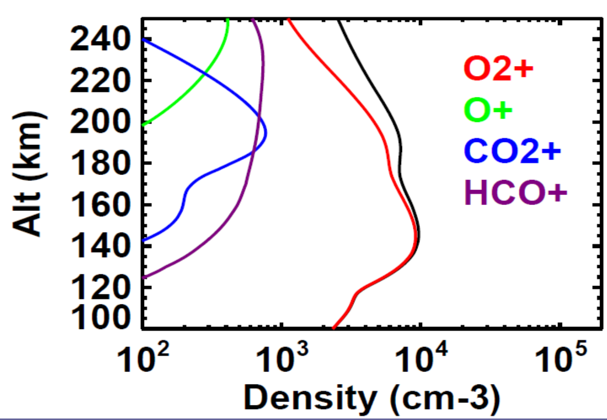

Figure 10. Model results for solar minimum near-terminator conditions (solar zenith angle ~80°) showing a bulge forming between 180 and 200 km as a result of HCO^+ and CO_2^+ buildup. Many other ions of lower densities are included in this simulation and are not shown here for clarity. Electron density is shown in black. The BU model is described most recently in Mendillo et al., [2011]; Lollo et al., [2012] and Matta et al. [2013a, b].

Electrons precipitating from the solar wind will impact the upper atmosphere and may have sufficient energy to ionize local neutral species. Solar wind electrons have access to topside ionospheric plasma, making them key candidates for sources of plasma enhancement at the altitude of the bulge. A preliminary look at the contribution of electron precipitation ionization using observations and modeling is shown in Figure 11. The precipitating electron ionization rate was calculated using a kinetic model [*Lillis et al.*, 2009] and compared with photo-ionization rates in the BU ionospheric model [*Martinis et al.*, 2003; *Mendillo et al.*, 2011; *Matta et al.*, 2013a, b].

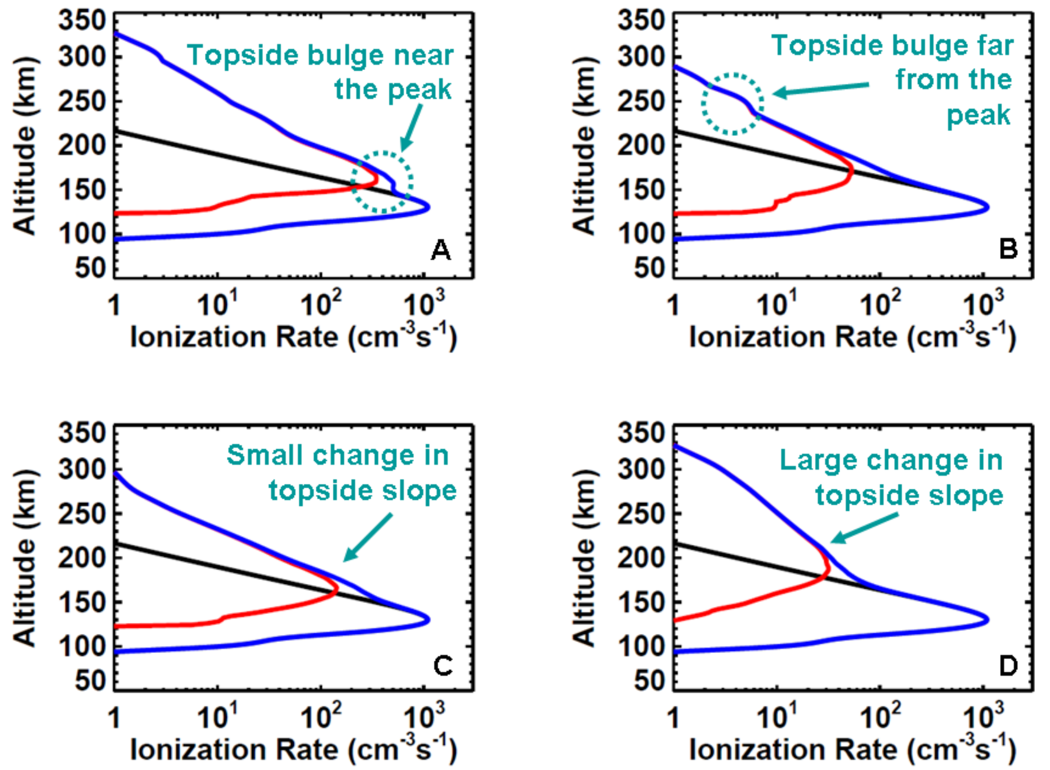

Figure 11. Ionization rates as a function of altitude of photo-ionization sources from fluid model (black line) and for precipitating electrons from kinetic model (red line) for various conditions. The blue line is the sum of ionization rates. In all panels, the slope of the topside ionosphere in blue shows relative contributions of the electron precipitation ionization rate. In the top row, bulges appear at varying altitudes, widths and magnitudes. In the bottom row, electron precipitation does not form a distinct bump or layer, but alters the topside scale height (slope) of the electron density profiles. These features have been classified according to their observed occurrence rates by Withers et al. [2012]. Preliminary examination indicates that electron precipitation can contribute to the observed variability in the topside ionosphere. These figures were generated for solar minimum conditions with a solar zenith angle of 67°.

In this Task, an existing ionospheric model previously developed at BU (e.g., [*Matta et al.*, 2013b]) as well as output from another kinetic model (e.g., [*Lillis et al.*, 2009]) that has already been delivered to the Co-I by collaborator Lillis, will be used in conjunction to interpret the bulge characteristics by examining chemical and solar drivers as follows:

Step D.1 – Calculate modeled properties of the sunset bulge due to chemical processes.
Step D.2 – Determine the timescale of chemical recombination for sunset bulge.
Step D.3 – Calculate total ionization rates using ionospheric model combined with ionization from the kinetic model.
Step D.4 – Determine modeled timescale of solar wind precipitation formed bulge.
Step D.5 – Calculate transport velocities due to bulge-induced gradients from model.
Step D.6 – Derive the temporal variation in bulge features, and dissipation timescales. Determine effects of each process on the variations in transport and related effects on modeled ion escape flux.

Step D.7 – Compare model results to observations for bulge feature properties (altitude, magnitude, width, timescale, and local as well as magnetic field conditions) to determine the potential of each mechanism to enhance topside plasma.

The results from the steps of this Task will contribute to interpreting the observations by examining two possible sources of topside plasma enhancements. Calculations of escape fluxes derived by the model will be compared with similar calculations from observations to determine the relative importance of each mechanism. The conclusions will also be useful in forming a predictive framework for future observations.

9 – Anticipated Results

Archived MGS and MEX daytime measurements of the topside ionosphere of Mars will have been thoroughly examined to identify the characteristics of topside ionospheric bulges. Analysis of observed properties and sources are anticipated to result in improving our understanding of the topside ionosphere by determining the variability of the bulge with local and solar conditions. The observed timescale and magnitude of the bulge feature will be examined to calculate perturbations in transport and thermal escape velocities for the first time for the topside ionosphere of Mars. Subsequent effects on escape fluxes of hydrogen-containing ions (HCO^+ and HCO_2^+) as well as the effects of varying chemical composition in the topside ionosphere will be determined.

At least two papers will be submitted for peer-review as a result of this study. A manuscript will report the characteristics of the observed topside bulge feature derived from the work in Tasks A and B. A second manuscript will discuss the possible contribution of chemical and solar source mechanisms in producing the topside, and will describe the variability in transport velocities from the results of Task D. If the analysis in Task C reveals inter-instrument nuances that can benefit the science community, then an additional manuscript describing those results will also be submitted.

10 – Relevance to NASA

NASA’s objectives for Mars are to study its climate, geological evolution and habitability. The Mars Data Analysis Program objectives are to ‘… enhance scientific return from missions to Mars…’, and the Mars Exploration Program Analysis Group (MEPAG) 2010 Science Goals emphasize the need to characterize the plasma structure and dynamics in the atmosphere of the planet [MEPAG, 2010 – Goal II.A.1]. Also highlighted is the need to characterize the availability of water during evolving atmospheric conditions [MEPAG – Goal I.C.3]. We will contribute to these goals by utilizing three instrument datasets to improve our understanding of the Martian climate by addressing variability and possible sources of a key region of its atmosphere. These investigations are critical to understanding atmospheric escape and impact the evolution of water. The outcome of these investigations will serve the scientific community further by helping shape questions to be addressed by the imminent Mars Atmosphere and Volatile Evolution (MAVEN) mission.

The goals of the work described here lead up to interpretation of model results that fall under the high-priority research umbrella identified by the MDAP 2013 NRA. A useful application of the modeling outcome is to predict how variability in the topside ionosphere affects water escape and how enhanced topside plasma densities affect inter-spacecraft radio communications, benefiting mission control applications. Each of the datasets used in this work is publicly archived. We will not be using any MEX topside sounder or radio occultation data that were not made publicly available 30 days prior to the submission deadline of this proposal, conforming to MDAP requirements.

11 – Personnel

The study will be conducted by PI Paul Withers, Co-I Majd Matta, and an undergraduate student at Boston University. Collaborators David Morgan (University of Iowa) and Collaborator Robert Lillis (UC Berkeley) will provide advice as needed.

Institutional PI: Paul Withers is a Professor of Astronomy at Boston University. He has extensive experience accessing and analyzing MGS and MEX datasets that will be used for this project. He will be responsible for directing the Co-I to oversee the success of the investigations, provide advice when needed, and to ensure compliance with all reporting requirements. Paul's research includes studying the behavior of the Martian upper atmosphere and ionosphere and analysis of accelerometer data.

Science PI/Co-I: Majd Matta recently completed doctoral work on the ionosphere of Mars, investigating the composition, thermal structure and dynamics of plasma [*Matta* 2013, PhD Thesis]. As a postdoctoral researcher at Boston University, Majd will be available to work on this project and as the science lead. Responsibilities include training an undergraduate student to use the data processing tools.

Collaborator: Dr. David Morgan is the MARSIS Project Manager at the University of Iowa. He will provide feedback, when needed, on the development and validation of the techniques used to identify the topside bulge feature in ionograms. Dave has authored over a dozen papers and presentations on the results of the MARSIS topside sounder and his research interests lie in studying the upper ionosphere.

Collaborator: Dr. Robert Lillis is an Assistant Research Physicist in the space physics research group at the UC Berkeley Space Sciences Laboratory. Rob has developed the kinetic code that provides quantities necessary for the modeling task of this work. His involvement will be to provide feedback, as needed, regarding the mechanics of the kinetic model. Rob's research interests include upper atmospheric variability at Mars.

12 – Work Plan

This study will be carried out by Majd Matta, and it will include interacting with the PI and collaborators and student training. Professor Paul Withers will supervise the study to ensure its compliance with all program requirements. His funded effort is 1 week but a larger portion of his time during the academic year will be available for mentoring the

Co-I in this project. He will be available to provide support for the tools that convert frequency residuals into electron density profiles when necessary. An undergraduate student will be trained to run the automated tools and to validate results with observations. Collaborator Morgan will advise us on the inversions of MARSIS topside sounder data and will spend 1-2 days each year on these interactions. Collaborator Lillis will advise us on the kinetic modeling used to derive electron precipitation ionization rates as needed, with a commitment of ~1 day per year. Interactions with collaborators will occur over email and the phone. Face-to-face meetings with the collaborators will occur at conference meetings and MAVEN team meetings that the proposal team members commonly attend.

The timeline for completion of the action items described in the Tasks is shown in Table 1. Majd Matta will take the lead in preparing the resulting manuscripts. An integral component of professional development will be to disseminate the results of this work at conferences (none in the first year, and one for each of the second and third years) in order to get feedback on the intermediate efforts. The working group meeting most beneficial to this type of research is the annual Mars Upper Atmosphere Meeting that the Co-I has been an active member of since 2009 [*Opgenoorth et al.*, 2010]. This meeting will be budgeted for the second year. Majd will also present the results of this work at the annual DPS meeting (budgeted for the third year) to reach a broader science audience.

Table 1. Timeline for plan of work.

	Milestones, Efforts and Deliverables
Year 1	• Co-I trains undergraduate student on data processing tools (0.5 months). • Student processes MGS and MEX radio occultation data while Co-I Matta automates MARSIS ionogram inversion (3 months). PI Withers provides developed radio occultation data extraction tools. Collaborator Morgan provides MARSIS data inversion advice as needed. *Steps A.1-A.4.*
Year 2	• Student processes MARSIS data while Co-I Matta performs statistical analysis and correlations for processed MGS & MEX radio occultation data (2 months). S*teps A.5 and B.1-B.2.* Co-I Matta begins to draft data analysis manuscript. • Student manually process observations that slipped automatic detection while Co-I completes statistical analysis and correlations for MARSIS topside sounder dataset, determines transport velocity variations from observations, and appends data analysis manuscript draft (1 month). *Steps A.6 and B.3-B.4.* • Co-I completes manuscript on data analysis, attends first meeting (0.5 months).
Year 3	• Co-I compares and interprets differences in instrumental techniques (0.5 months). *Step C.1.* • Co-I runs model simulations, interprets results, and drafts manuscript for interpretation of model results (2.5 months). Collaborator Lillis provides feedback on kinetic model tool as needed. *Steps D.1- D.7.* • Co-I completes manuscript on interpreting results from model and observations, attends second meeting (0.5 months).

References

Arkani-Hamed, J. (2004), A coherent model of the crustal magnetic field of Mars, *J. Geophys. Res.*, 109, E09005, doi:10.1029/2004JE002265.

Bougher, S. W., S. Engel, R. G. Roble, and B. Foster (2000), Comparative terrestrial planet thermospheres, 3, Solar cycle variation of global structure and winds at solstices, *J. Geophys. Res.*, 105, p. 17,669–17,692.

Duru, F., D. A. Gurnett, T. F. Averkamp, D. L. Kirchner, R. L. Huff, A. M. Persoon, J. J. Plaut, and G. Picardi (2006), Magnetically controlled structures in the ionosphere of Mars, *J. Geophys. Res.*, 111, A12204, doi:10.1029/2006JA011975.

Fallows, K., P. Withers and Z. Girazian (2011), Variability in the M1 Layer of the Martian Ionosphere, American Geophysical Union, Fall Meeting 2011, abstract #SA13A-1880.

Fox, J. L. (2003), Effect of H_2 on the Martian ionosphere: Implications for atmospheric evolution, *J. Geophys. Res.*, 108(A6), 1223, doi:10.1029/2001JA000203.

Fox, J. L. and K. E. Yeager (2006), Morphology of the near-terminator Martian ionosphere: A comparison of models and data, *J. Geophys. Res.*, 111, A10309, doi:10.1029/2006JA011697.

Gurnett, D. A., D.L. Kirchner, R. L. Huff, D. D. Morgan, A.M. Persoon, T.F. Averkamp, F. Duru, E. Nielsen, A. Safaeinili, J.J. Plaut, G. Picardi (2005), Radar Soundings of the Ionosphere of Mars, *Science*, 310, p. 1929 – 1933, doi: 10.1126/science.1121868.

Hanson, W.B., S. Sanatani and D.R. Zuccaro (1977), The Martian ionosphere as observed by the Viking retarding potential analyzers, *J. Geophys. Res.*, 82, pp. 4351–4363.

Kim, E., H. Seo, J. Kim, J. Lee, Y. Kim, G.-H. Choi and E.-S. Sim (2012), The Analysis of the Topside Additional Layer of Martian Ionospher Using MARSIS/Mars Express Data, *J. Astron. Space Sci.*, 29 (4), p. 337 – 342, http://dx.doi.org/10.5140/JASS.2012.29.4.337

Kopf, A. J., D. A. Gurnett, D. D. Morgan, and D. L. Kirchner (2008), Transient layers in the topside ionosphere of Mars, *Geophys. Res. Lett.*, 35, L17102, doi:10.1029/2008GL034948.

Krasnopolsky, V.A. (2002), Mars' upper atmosphere and ionosphere at low, medium, and high solar activities: implications for evolution of water, *J. Geophys. Res.*, 107, 5128, doi:10.1029/2001JE001809.

Krasnopolsky, V.A. and P.D. Feldman (2001), Detection of molecular hydrogen in the atmosphere of Mars, *Science*, 294, p. 1914–1917.

Krymskii, A. M., T. K. Breus, N. F. Ness, M. H. Acun˜a, J. E. P. Connerney, D. H. Crider, D. L. Mitchell, and S. J. Bauer (2002), Structure of the magnetic field fluxes connected with crustal magnetization and topside ionosphere at Mars, *J. Geophys. Res.*, 107(A9), 1245, doi:10.1029/2001JA000239.

Lillis, R. J., D. L. Mitchell, R. P. Lin and M. H. Acuña (2008), Electron reflectometry in the martian atmosphere, *Icarus*, 9194, p. 544 – 561.

Lillis, R. J., M. O. Fillingim, L. M. Peticolas, D. A. Brain, R. P. Lin, and S. W. Bougher (2009), Nightside ionosphere of Mars: Modeling the effects of crustal magnetic fields and electron pitch angle distributions on electron impact ionization, *J. Geophys. Res.*, 114, E11009, doi:10.1029/2009JE003379.

Lollo A., P. Withers, K Fallows, Z. Girazian, M. Matta, P.C. Chamberlin (2012), Numerical simulations of the ionosphere of Mars during a solar flare, *J. Geophys. Res.*, 117 (A5), A05314, doi: 10.1029/2011JA017399.

Lundin, R., E. Dubinin, H. Koskinen, O. Norberg, N. Possarenko and S. Barabash (1991), On the momentum transfer of the solar wind to the Martian topside ionosphere, *Geophy. Res. Lett.*, 18 (6), p. 1059 – 1062.

Martinis, C. R., J. K. Wilson, and M. J. Mendillo, MMartinis, C. R., J. K. Wilson, and M. J. Mendillo, Modeling day-to-day ionospheric variability on Mars, *J. Geophys. Res.*, 108(A10), 1383, doi:10.1029/2003JA009973, 2003.

Ma, Y.-J., and A. F. Nagy (2007), Ion escape fluxes from Mars, *Geophys. Res. Lett.*, 34, L08201, doi:10.1029/2006GL029208.

Matta, M., Modeling the Martian Ionosphere, Ph.D. thesis, Boston University, Boston, 2013.

Matta, M., P. Withers, M. Mendillo (2013a), The Composition of Mars' Topside Ionosphere: Effects of Hydrogen, *J. Geophys. Res.,* 118, p. 2681–2693, doi: 10.1002/jgra.50104.

Matta, M., M. Galand, L. Moore, M. Mendillo and P. Withers (2013b), Numerical Simulations of Ion and Electron Temperatures in the Ionosphere of Mars: Multiple Ions and Diurnal Variations, *Icarus*, in press, available online at http://www.sciencedirect.com/science/article/pii/S0019103513003862.

Mendillo, M. and P. Withers (2008), Solar Flare Effects Upon the Ionospheres of Earth and Mars, *Radio Sounding and Plasma Physics*, CP974, p. 58-70.

Mendillo, M., A. Lollo, P. Withers, M. Matta, M. Pätzold, and S. Tellmann (2011), Modeling Mars' ionosphere with constraints from same-day observations by Mars Global Surveyor and Mars Express, *J. Geophys. Res.*, 116, A11303, doi:10.1029/2011JA016865.

MEPAG (2010), Mars Scientific Goals, Objectives, Investigations, and Priorities: J.R. Johnson, ed., 49 p. white paper posted September, 2010 by the Mars Exploration Program Analysis Group (MEPAG) at http://mepag.jpl.nasa.gov/reports/index.html.

Moore, L., P. Withers, K. Cahoy, I. Beerer, R. Hu, K. Kennedy, R. Kingsbury, and M. Webber (2012), Development and validation of software to process radio occultation data: From time series of frequency residuals to vertical profiles of atmospheric and ionospheric properties, Fall AGU, 3-7 December 2012.

Nagy, A.F., Cravens, T.E. Solar system ionospheres, in: Mendillo, M., Nagy, A.F., Waite, J.H. (Eds.), Atmospheres in the Solar System: Comparative Aeronomy. American Geophysical Union, Washington, DC, pp. 39–54, 2002.

Ness, N., Acuña M., Connerney J., Kliore A., Breus T., Krymskii A., Cloutier P., Bauer S. (2000), Effects of magnetic anomalies discovered at Mars on the structure of the Martian ionosphere and solar wind interaction as follows from radio occultation experiments, *Journal of Geophysical Research*, 105, p. 15991–16004.

Nier, A. O., and M. B. McElroy (1977), Composition and structure of Mars' upper atmosphere – Results from the neutral mass spectrometers on Viking 1 and 2, *J. Geophys. Res.*, 82, 4341–4349.

Opgenoorth, H., O. Witasse and P. Withers (2010), Mars Upper Atmosphere Network, American Astronomical Society, 42nd DPS meeting, Abstract #30.10, p. 1029.

Pätzold, M. , P. Withers, S. Tellmann, M. Mendillo, K. Peter, B. Häusler, D. Hinson and L. Tyler (2007), American Geophysical Union, Fall Meeting, Abstract #P32A-01.

Schunk, R.W. and A.F. Nagy (2009), *Ionospheres,* 2nd ed. Cambridge University Press, New York.

Shinagawa, H. and T. E. Cravens (1989*),* A one dimensional multispecies magneto hydrodynamic model of the dayside ionosphere of Mars, *J. Geophys. Res.*, 94(A6), p.6506–6516*,* doi:10.1029/JA094iA06p06506.

Shinagawa, H. and T. Cravens (1992), The Ionospheric Effects of a Real Intrinsic Magnetic Field at Mars, *J. Geophys. Res.*, 97 (E1), p. 1027-1035.

Shizgal, B. and G. Arkos (1996), Nonthermal escape of the atmospheres of Venus, Earth, and Mars, *Revs. Geophys.*, 34, 4, p. 483 – 505.

Wang, J.-S., and E. Nielsen (2003) , Wavelike structures in the Martian topside ionosphere observed by Mars Global Surveyor, *J. Geophys. Res.*, 108(E7), 5078, doi:10.1029/2003JE002078.

Withers, P. (2009), A review of observed variability in the dayside ionosphere of Mars, *Adv. Space Res.*, 44, 3, p. 277-307.

Withers, P., et al. (2012), A clear view of the multifaceted dayside ionosphere of Mars, *Geophys. Res. Lett.*, 39, L18202, doi:10.1029/2012GL053193.

Withers, P., L. Moore, K. Cahoy and I. Beerer (2013), How to process radio occultation data: 1. From time series of frequency residuals to vertical profiles of atmospheric and ionospheric properties, *Planet. Space Science*, under review.

Zou, H., E. Nielsen, J.-S. Wang and X.-D. Wang (2010), Reconstruction of nonmonotonic electron density profiles of the Martian topside ionosphere, *Planet. Space Sci.*, 58, p. 1391 – 1399.

Biographical Sketch for PI Paul Withers

Astronomy Department
Boston University
725 Commonwealth Avenue
Boston MA 02215

Tel: (617) 353 1531
Fax: (617) 353 6463
Email: withers@bu.edu
Citizenship: British (Green Card holder)

Education

- PhD, Planetary Science, University of Arizona — 2003
- MS, Physics, Cambridge University, Great Britain — 1998
- BA, Physics, Cambridge University, Great Britain — 1998

Professional Experience

- Assistant Professor, Astronomy Department (Boston Univ.) — 2010-present
- Senior research associate — Dr. Michael Mendillo (Boston Univ.) — 2007 – 2010
  Research associate — Dr. Michael Mendillo (Boston Univ.) — 2003 – 2007
  Analysis of ionospheric data from Venus, Mars and Earth, plus numerical modeling
- Graduate research assistant — Dr. Stephen Bougher (Univ. of Arizona) — 1998 – 2003
  Studied tides in the martian upper atmosphere. Played an advisory role in mission operations for Mars Global Surveyor and Mars Odyssey aerobraking

Selected Fellowships, Honors, and Awards

- NASA Early Career Fellowship — 2009
- CEDAR Postdoctoral Fellowship from NSF for upper atmospheric research — 2003
- Kuiper Memorial Award from the University of Arizona for excellence in academic work and research in planetary science — 2002
- Nominated for the Meteoritical Society/Geological Society of America's Best Student Paper in Planetary Sciences Award — 2002

Mission Involvement

- JPL Critical Data Products provider for MAVEN and Curiosity
- Atmospheric Advisory Group participant for atmospheric flights of MGS, Odyssey, Spirit, Opportunity, Curiosity
- Co-Investigator on ExoMars Entry Demonstrator Module Entry Science Investigation, Venus Express Accelerometer, Venus Express Radio Science, Mars Express Radio Science, Huygens Atmospheric Structure Investigation
- Archived atmospheric data for Odyssey, Spirit, Opportunity, Phoenix; coordinated archiving of Venera 15/16 ionospheric data

Selected Peer Reviewed Publications

- **Withers**, Fillingim, Lillis, Haeusler, Hinson, Tyler, Paetzold, Peter, Tellmann, and Witasse (2012) Observations of the nightside ionosphere of Mars by the Mars Express Radio Science Experiment MaRS, Journal of Geophysical Research, 117, A12307, doi:10.1029/2012JA018185
- **Withers**, Fallows, Girazian, Matta, Haeusler, Hinson, Tyler, Morgan, Paetzold, Peter, Tellmann, Peralta, and Witasse (2012) A clear view of the multifaceted dayside ionosphere of Mars, Geophysical Research Letters, 39, L18202, doi: 10.1029/2012GL053193
- *Lollo*, **Withers**, Fallows, Girazian, Matta, and Chamberlin (2012) Numerical simulations of the ionosphere of Mars during a solar flare, Journal of Geophysical Research, 117, A05314, doi:10.1029/2011JA017399
- Sheel, Haider, **Withers**, Kozarev, Jun, Kang, Gronoff, and Simon Wedlund (2012) Numerical simulation of the effects of a solar energetic particle event on the ionosphere of Mars, Journal of Geophysical Research, 117, A05312, doi:10.1029/2011JA017455
- Mendillo, *Lollo*, **Withers**, Matta, Paetzold, and Tellmann (2011) Modeling Mars' ionosphere with constraints from same-day observations by Mars Global Surveyor and Mars Express, Journal of Geophysical Research, 116, A11303, doi:10.1029/2011JA016865
- **Withers**, *Pratt*, Bertaux, and Montmessin (2011) Observations of thermal tides in the middle atmosphere of Mars by the SPICAM instrument, Journal of Geophysical Research, 116, E11005, doi:10.1029/2011JE003847
- **Withers** (2009) A review of observed variability in the dayside ionosphere of Mars, Advances in Space Research, 44, 277-307
- **Withers**, Mendillo, Hinson, and Cahoy (2008) Physical characteristics and occurrence rates of meteoric plasma layers detected in the martian ionosphere by the Mars Global Surveyor Radio Science Experiment, Journal of Geophysical Research, 113, A12314, doi:10.1029/2008JA013636
- **Withers** (2008) Theoretical models of ionospheric electrodynamics and plasma transport, Journal of Geophysical Research, 113, A07301, doi:10.1029/2007JA012918
- Mendillo, **Withers,** Hinson, Rishbeth, and Reinisch (2006) Effects of solar flares on the ionosphere of Mars, Science, 311, 1135-1138
- Bougher, Bell, Murphy, Lopez-Valverde, and **Withers** (2006) Polar warming in the Mars thermosphere: Seasonal variations owing to changing insolation and dust distributions, Geophysical Research Letters, 33, L02203, doi:10.1029/2005GL024059
- **Withers** (2006) Mars Global Surveyor and Mars Odyssey Accelerometer observations of the martian upper atmosphere during aerobraking, Geophysical Research Letters, 33, L02201, doi:10.1029/2005GL024447
- **Withers** and Mendillo (2005) Response of peak electron densities in the martian ionosphere to day-to-day changes in solar flux due to solar rotation, Planetary and Space Science, 53, 1401-1418, doi:10.1016/j.pss.2005.07.010
- **Withers**, Mendillo, Rishbeth, Hinson, and Arkani-Hamed (2005) Ionospheric characteristics above martian crustal magnetic anomalies, Geophysical Research Letters, 32, L16204, doi:10.1029/2005GL023483
- **Withers**, Bougher, and Keating (2003) The effects of topographically-controlled thermal tides in the martian upper atmosphere as seen by the MGS Accelerometer, Icarus, 164**,** 14-32

Biographical Sketch for Co-I Majd Matta

Center for Space Physics — Tel: (617)-353-5990
Boston University — Email: majdm@bu.edu
725 Commonwealth Ave., Boston, MA 02215 — Citizenship: US

Education

- PhD, Astronomy, Boston University 2013
- MA, Astronomy, Boston University 2009
- BS, Physics, University of Massachusetts Boston 2006
- BE, Computer Engineering, American University of Beirut, Lebanon 1998

Research Experience

- Postdoctoral Researcher Prof. John Clarke, Boston University 2013 – Present
  Observing the upper atmosphere of Mars using HST and MAVEN – IUVS
- Graduate Research Assistant Prof. Michael Mendillo and Paul Withers 2009 – 2013
  Modeling the composition, thermal structure and crustal field region dynamics in the ionosphere of Mars
- Graduate Research Assistant Prof. Michael Mendillo 2007 – 2009
  Observing and characterizing extended lunar sodium tail using all-sky-cameras
- Graduate Research Assistant Prof. Meers Oppenheim 2006 – 2007
  Particle-in-cell studies of plasma motion in magnetic fields

Publications

- **Matta, M.**, M. Galand, L. Moore, M. Mendillo and P. Withers (2013), Numerical simulations of ion and electron temperatures in the ionosphere of Mars: multiple ions and diurnal variations, *Icarus*, in press, http://dx.doi.org/10.1016/j.icarus.2013.09.006.
- Mendillo, M., C. Navaez, P. Withers, **M. Matta**, W. Kofman and J. Mouginot (2013), Variability in Ionospheric Total Electron Content at Mars, *Planet. Sp. Science*, in press.
- **Matta, M.**, P. Withers, M. Mendillo (2013), The Composition of Mars' Topside Ionosphere: Effects of Hydrogen, *J. Geophys. Res.,* 118, p. 2681–2693, doi: 10.1002/jgra.50104
- Withers, P., K. Fallows, Z. Girazian, **M. Matta**, B. Häusler, D. Hinson, L. Tyler, D. Morgan, M. Pätzold, K. Peter, S. Tellmann, J. Peralta, and O. Witasse (2012), A clear view of the multifaceted dayside ionosphere of Mars, *Geophys. Res. Lett.*, 39, L18202, doi:10.1029/2012GL053193
- Lollo A., P. Withers, K Fallows, Z. Girazian, **M. Matta**, P.C. Chamberlin (2012), Numerical simulations of the ionosphere of Mars during a solar flare, *J. Geophys. Res.*, 117 (A5), A05314, doi: 10.1029/2011JA017399.
- Michael Mendillo, Anthony Lollo, Paul Withers, **Majd Matta**, Martin Pätzold, and Sylvia Tellmann (2011), Modeling Mars' Ionosphere with Constraints from Same-Day Observations by Mars Global Surveyor and Mars Express, *J. Geophys. Res.*, 116 (A11), doi:10.1029/2011JA016865.
- **M. Matta**, S. Smith, J. Wilson, J. Baumgardner, M. Mendillo (2009), The sodium tail of the Moon, *Icarus*, 204 (2), p. 409-417.

Current and Pending Support for PI Paul Withers

Current Support

Principal Investigator: Paul Withers
Project/Proposal Title: Radio occultation studies at Mars
Source of Support: NASA Early Career Fellowship Program
Award: NNX13AH89G
Award Amount (or Annual Rate): $99,999 Period Covered: 03/2013-03/2015
Person Months Committed to Project per year: Cal: Acad: Summ: 0.45

Principal Investigator: Paul Withers
Project/Proposal Title: Meteoric plasma layers on Venus and Mars
Source of Support: NASA Planetary Atmospheres Program
Award: NNX13AH11G
Award Amount (or Annual Rate): $232,000 Period Covered: 03/2013-02/2016
Person Months Committed to Project per year: Cal: Acad: Summ: 0.50

Principal Investigator: Paul Withers
Project/Proposal Title: EDL reconstruction for MSL
Source of Support: NASA/JPL
Award: 1472312
Award Amount (or Annual Rate): $199,497 Period Covered: 12/2012-09/2014
Person Months Committed to Project per year: Cal: Acad: Summ: 1.00

Principal Investigator: Paul Withers
Project/Proposal Title: The vertical structure of the Venus ionosphere and its implications for terrestrial planet ionospheres (Zachary Girazian graduate fellowship)
Source of Support: NASA Earth and Space Science Fellowship (NESSF) Program
Award: NNX12AN03H
Award Amount (or Annual Rate): $90,000 Period Covered: 09/2012-08/2015
Person Months Committed to Project per year: Cal: Acad: Summ:0.00

Principal Investigator: Paul Withers
Project/Proposal Title: Modeling day-to-day variability in the ionosphere of Venus (Katy Fallows graduate fellowship)
Source of Support: NASA Earth and Space Science Fellowship (NESSF) Program
Award: NNX12AN80H
Award Amount (or Annual Rate): $90,000 Period Covered: 09/2012-08/2015
Person Months Committed to Project per year: Cal: Acad: Summ:0.00

Principal Investigator: Paul Withers
Project/Proposal Title: The ionosphere of Venus
Source of Support: NSF Astronomy and Astrophysics Research Grants (AAG) Program
Award: 1211490
Award Amount (or Annual Rate): $294,211 Period Covered: 08/2012-07/2015
Person Months Committed to Project per year: Cal: Acad: Summ: 1.00

Principal Investigator: Paul Withers
Project/Proposal Title: Exploring the ionosphere of Mars
Source of Support: NASA Mars Data Analysis Program
Award: NNX12AJ39G
Award Amount (or Annual Rate): $159,393 Period Covered: 05/2012-05/2015
Person Months Committed to Project per year: Cal: Acad: Summ: 0.50

Principal Investigator: Paul Withers
Project/Proposal Title: Integration of MAVEN neutral and plasma observations
Source of Support: NASA MAVEN Participating Scientist Program
Award: Pending
Award Amount (or Annual Rate): $284,243 Period Covered: 11/2013-04/2016
Person Months Committed to Project per year: Cal: Acad: 1.80 Summ: 0.00

Pending Support

Principal Investigator: Paul Withers
Project/Proposal Title: Atmospheric conditions for InSight
Source of Support: NASA/JPL Mars Critical Data Products Program
Award: Pending
Award Amount (or Annual Rate): $216,133 Period Covered: 09/2013-08/2016
Person Months Committed to Project per year: Cal: Acad: Summ: 0.50

Principal Investigator: Paul Withers
Project/Proposal Title: CAREER: Magnetic mysteries at Mars
Source of Support: NSF CAREER Program
Award: Pending
Award Amount (or Annual Rate): $743,347 Period Covered: 01/2014-12/2018
Person Months Committed to Project per year: Cal: Acad: Summ: 0.50

Principal Investigator: Paul Withers
Project/Proposal Title: Cottrell Scholarship
Source of Support: Research Corporation for Science Advancement
Award: Pending
Award Amount (or Annual Rate): $75,923 Period Covered: 09/2014-08/2016
Person Months Committed to Project per year: Cal: Acad: Summ: 0.00

Current and Pending Support for Co-I Majd Matta

Current Support:
No current support

Pending Support:
No pending support